physica status solidi b
www.pss-b.com

Initial Stages of Palladium Growth on Vicinal Si(001)-(2×1) Surfaces

Sandhya Chandola, Norbert H. Nickel, Julian Plaickner, Karsten Hinrichs, Jörg Rappich, and Norbert Esser**

The early growth stages of palladium (Pd) on Si(001) are studied in situ by reflectance anisotropy spectroscopy and Raman spectroscopy in ultrahigh vacuum. Two vicinal Si(001) samples with different degrees of surface ordering are investigated, revealing a distinct Volmer–Weber-type growth behavior. Ex situ atomic force microscopy shows an inhomogeneous surface covered with islands on the less-ordered substrate, while a complex layer with circular structures related to a nucleation-controlled phase transition as previously reported is found on the well-ordered sample. By Raman spectroscopy, a silicide-like reacted phase at the Si–Pd interface is identified which is promoted by annealing up to 600 °C. The appearance of several additional phonon modes due to the interface reaction is in very good agreement with vibrational modes obtained from ab initio calculations for Pd incorporation into Si surface layers.

1. Introduction

Thin films of transition metal silicides have been used as interconnects in microelectronics devices for decades due to their low resistivity and good thermal stability.[1–3] Among the large number of silicides used in metal–silicon interconnects, palladium (Pd)-based silicides have several advantages due to the low formation temperature and ease of formation. Beyond their role in the semiconductor industry, Pd silicides have become important compounds for catalytic applications and there is intense research to improve the catalytic activity, selectivity, and stability of Pd to promote specific reactions. For example, Pd-based catalysts are used in hydrogenation of C_2H_2 to C_2H_4 due to their high activity for acetylene conversion.[4] Low coverages of Pd on metal surfaces have shown significant enhancement of catalytic reactions, and this effect has been explained by geometric and/or electronic effects, with the isolated Pd sites acting as active sites.[5]

As an alternative to conventional 3D powder catalysts, thin Pd films on various substrates such as silicon have been tested in the hydrogenation of acetylene.[6] However, the catalytic activity has been found to be drastically reduced due to the formation of palladium silicide. Pd is known to form different phases of silicide structures on Si.[7] Pd_2Si formed on Si(111) is epitaxial, whereas it is polycrystalline when grown on Si(001), with random azimuth orientations.[8,9] At coverages below 1 ML, Pd is known to react with Si(001) at room temperature (RT) and forms Pd–Si bonds, while at coverages above 1 ML, a Pd_2Si-like compound is formed at the interface.[10–12] Only one primary phase is formed below 700 °C: hexagonal Pd_2Si.[8] PdSi is usually formed above the eutectoid temperature (≈800 °C).[11] At longer annealing times, PdSi can also coexist with Pd_2Si over a large temperature range.[13] A model calculation for different interface geometries of the Si(111)–Pd_2Si interface showed that at low Pd coverages, epitaxial growth does not occur at the beginning of the deposition.[14] The only interface geometry which agreed with the experimental data at low coverages was the one formed by interstitial Pd atoms below the Si surface. On increasing Pd coverage, the concentration of these clusters increases. However, the Pd/Si(001) interface studied here has not been analyzed in so much detail due to its complex, nonepitaxial growth.

The focus of this paper is to investigate the initial interactions at the interface between Pd and vicinal Si(001) in ultrahigh vacuum (UHV) to understand the precursor formation of silicide-like structures. The interactions are investigated in situ, by monitoring the structural modifications of the vicinal Si(001) surface at very low Pd coverages with reflectance anisotropy spectroscopy (RAS) and Raman spectroscopy. Additional ex situ investigations after growth are performed by Raman, RAS, and AFM in air.

Vicinal Si(001) surfaces with a well-defined step structure are chosen as a substrate as it is well known that the morphology of a surface, such as structure and orientation, can play major roles in surface processes such as nucleation in growth or catalysis.[15,16] These stepped surfaces can be useful model systems to mimic

S. Chandola, N. H. Nickel, K. Hinrichs, J. Rappich
Nanoscale Solid-Liquid Interfaces
Helmholtz-Zentrum Berlin für Materialien und Energie
Schwarzschildstr. 8, 12489 Berlin, Germany
E-mail: sandhya.chandola@helmholtz-berlin.de

J. Plaickner, N. Esser
Institut für Festkörperphysik
TU Berlin
Hardenbergstr. 36, 10623 Berlin, Germany
E-mail: norbert.esser@tu-berlin.de

The ORCID identification number(s) for the author(s) of this article can be found under https://doi.org/10.1002/pssb.202400655.

DOI: 10.1002/pssb.202400655

certain aspects of catalytic reactions as they have been shown to influence the adsorption geometry and the decomposition paths of several hydrocarbon–substrate systems such as C_2H_2 on Pd surfaces.[17] RAS measurements of hydrogen on the Si(553)–Au surface have shown high reactivity of step sites to chemical reactions, where molecular hydrogen dissociates catalytically at the Si step edges.[18]

RAS is ideally suited to probe these reactive structures, since the anisotropy of the optical response can be directly related to the surface electronic structure. Moreover, Raman spectroscopy, applied to reconstructed or adsorbate modified surfaces, has been shown to be very sensitive to surface phonons, that is, vibrational modes, confined to a few atomic layers. In particular, in combination with ab initio calculations of vibrational modes, this has been proven to be a very versatile tool for surface structure analysis.[19,20] In this article, we show that this approach can successfully be applied to structurally complex interfaces such as Pd–Si.

2. Experimental and Theoretical Methods

RAS measurements were carried out in situ, to probe the change in the anisotropic optical properties of the surface during Pd deposition on Si(001). RAS measured the difference in reflectance R, at near normal incidence, of light linearly polarized in two orthogonal directions at the surface plane of a cubic material.[21] The RAS signal was defined by

$$\frac{\Delta R}{R} = \frac{R_{[\bar{1}10]} - R_{[110]}}{R} \tag{1}$$

where the directions $[\bar{1}10]$ and [110] correspond to directions parallel and perpendicular to the step edges, respectively. The RAS apparatus was similar to previously described setups.[22] RAS spectra in this work reported the real part of the anisotropy in the reflection coefficients $\Delta r/r$, which was related to the signal by $\Delta R/R = 2\mathrm{Re}(\Delta r/r)$.[22]

Raman spectroscopy measurements were also carried out in situ in the same UHV environment, but after the Pd deposition for subsequent annealing steps. The Raman measurements were obtained using a Dilor triple spectrometer and a Si-based high-efficiency charge-coupled device (CCD) detector. A solid-state laser with an excitation wavelength of 660 nm (≈1.9 eV) was used with a power of ≈250 mW. The Raman scattering intensity was measured in the parallel polarization configuration $z(yy)\bar{z}$, with y parallel to the steps in the $[\bar{1}10]$ direction, and z was along [001], perpendicular to the Si(001) surface. RAS and Raman spectroscopy were attached to an UHV analysis chamber with a base pressure of 1×10^{-10} mbar, which enabled the preparation of Si by direct current heating, deposition of metal adsorbates by effusion cells, and surface control via low-energy electron diffraction (LEED).

Si(001) substrates, with a miscut angle of 4° towards the [110] direction, were prepared from commercial n-type, *P*-doped Si(001) wafers (≈10 ohm-cm) and degassed in UHV for 12 h at 600 °C by direct current heating.

They were then cleaned by repeated flashing to 1150 °C, to obtain a predominantly single-domain (SD) (2×1) surface reconstruction. The anisotropic surface stress of the (2×1) dimer reconstruction results ideally in the formation of regularly arranged double steps separated by ≈4 nm wide SD (2×1) terraces. On real surfaces, preparation conditions and surface defects may lead to a less well-ordered structure comprising single and double atomic steps. This can be detected by RAS since single steps lead to dimer domains rotated by 90°. **Figure 1** shows typical RAS spectra of clean Si(001)-(2×1) surfaces.

The Pd structures were grown in situ by evaporating Pd from a high-temperature effusion cell onto the clean Si(001) surface held at RT. For vicinal surfaces, RAS is well suited to follow deposition/annealing cycles in situ. The coverage was given in monolayers (ML), with 1 ML corresponding to the surface atom density at the unreconstructed Si(001) surface (6.8×10^{14} atoms cm^{-2}). The Pd coverage was monitored by a quartz crystal oscillator, and the deposition rate was ≈0.1 ML min^{-1}. An infrared pyrometer with an accuracy of ±20 °C was used for monitoring the sample temperature. The pressure did not exceed 3×10^{-9} mbar during Pd evaporation. RAS monitored the deposition of Pd on the surface up to 2 ML and 4 ML coverage for the two cases discussed below. The "zero" position for RAS was defined by using an oxidized on-axis Si(001) sample, with an estimated error of $\pm 0.05 \times 10^{-3}$. After RAS of each Pd coverage at RT, Raman spectroscopy was performed and was followed by annealing from RT up to 600 °C. RAS was then measured again for the annealed samples after Raman. Moreover, the surface structure was analyzed by LEED after various deposition and annealing steps. After the in situ RAS and Raman measurements, the samples were removed from UHV, and ex situ AFM measurements were carried out by a Park Systems XE-100 instrument used in a noncontact mode.

Ab initio density functional theory calculations were performed to gain further insight into the interaction of Pd atoms with the silicon (001) surface. For this purpose, the Si(001)-(2×1) surface was modeled in a slab geometry with a vacuum region of 21 Å. The supercell consisted of up to 70 atoms, and the top three silicon layers were allowed to relax. For the calculations,

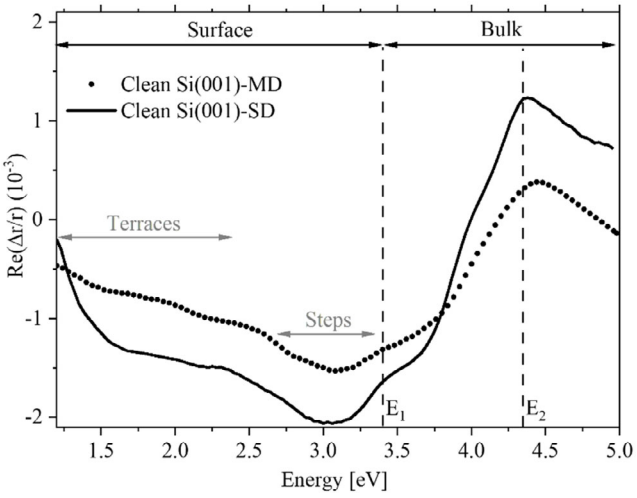

Figure 1. RAS of clean vicinal Si(001) surfaces with multi-domains (MD) and single-domains (SD). Black arrows show the energy range of surface and bulk transitions.

a Γ-centered k-point mesh of $3 \times 3 \times 1$ was used. To obtain equilibrium structures, ionic relaxations were carried out until the residual forces were equal or less than 10^{-3} eV Å. For the calculations, the Vienna Ab initio Simulation Package was used, and the generalized gradient approximation was employed.[23–25]

3. Results and Discussion-In-Situ Analysis

In this section, the results obtained from in situ RAS and Raman spectroscopy are presented. In Section 3.1, RAS data obtained from clean and Pd-covered Si(001) surfaces at RT, and then annealed up to 600 °C, will be presented. Section 3.2 will present Raman scattering results from the same samples as measured with RAS. In Section 3.3, ab initio calculations of the interface structure and vibrational modes are presented.

3.1. RAS

Before discussing the RAS measurements for the Pd coverages, a brief description of the typical spectroscopic fingerprints for the clean vicinal Si(001)-(2×1) surface is given. Figure 1 shows RAS of the clean Si(001) surface for both samples, with a broad negative feature at about 3 eV and a peak at 4.3 eV, similar to spectra obtained from other RAS studies of the surface.[26,27] The RAS spectra show the same general features, but with significantly different amplitudes which is indicative for a different domain ordering.

The optical anisotropy of the Si(001)-(2×1) surface originates from the structural anisotropy of the dimers and steps on the surface. Ab initio calculations of the RAS response for vicinal Si(001) have identified several key features.[28] The small shoulder at 3.4 eV and the peak at about 4.3 eV correspond to surface modified bulk optical transitions at the E_1 and E_2 critical points, respectively.[28] At energies lower than 3.4 eV, calculations have shown that the optical anisotropy is related to surface states from the Si dimers. At 3.0 eV, a minimum structure is observed which is related to dangling bonds at the double steps of the vicinal Si(001) surface.[28,29]

For energies greater than 3.4 eV, the anisotropic signal has been attributed to surface-induced bulk anisotropy.[28] The E_1 and E_2 structures have been shown to be sensitive to the anisotropic surface structure and the surface-induced stress extending into the bulk.[30,31]

The RAS spectra of the clean Si(001) surfaces are clearly dependent on surface preparation, displaying different magnitudes. A reduced domain imbalance gives rise to a smaller anisotropic signal because of partial cancelation of anisotropy from (1×2) and (2×1) domains. This multidomain (MD) surface comprises a mixture of single and double height atomic steps. A larger RAS amplitude originates from a greater single-domain (SD) ratio evidenced by the magnitude of the RAS signal below 3 eV from the step structure and surface contributions and above 3.4 eV from surface-induced bulk optical transitions.

The evolution and initial stages of reactions at the interface of Si(001) and Pd are monitored in situ with RAS as a function of the coverage from 0.5 to 4 ML in **Figure 2**a. The total anisotropy for both samples has reduced, compared to the spectrum of the clean Si(001) surfaces. Figure 2b shows RAS transients at three energies which provide information on the structural changes induced by Pd deposition. The signals at 2.5, 3, and 4.3 eV are related to surface-state related transitions, dangling bonds at the steps, and surface-induced bulk transitions respectively. The transients for the MD and SD samples show different surface modification processes during Pd growth. The surface states are initially quenched at a faster rate for the MD surface compared to the SD surface. This indicates that the growth morphology of Pd on the MD surface is different to the SD surface. STM studies have shown that Pd clusters agglomerate near the step edges with increasing Pd coverage, until the surface is covered by islands.[12] As the MD surface has a higher density of monoatomic steps which hinder surface diffusion, a greater number of Pd clusters nucleate and form 2D-like islands, strongly reducing the optical anisotropy from the Si surface. For the SD surface, there is still some residual optical anisotropy from Si surface and step related states even at 2 ML. This indicates that a larger area of the bare Si surface is exposed for the same Pd coverage. The RAS transients for the SD surface show that the signals from the surface and steps partially recover between 0.5 and 1 ML indicating agglomeration of the islands. According to STM and photoemission studies of Pd growth on Si(100),[10] Pd initially nucleates randomly on the dimer rows and grows as 3D islands (Volmer–Weber growth mode). This explains the residual optical anisotropy from the bare Si SD surface even for 2 ML Pd coverage due to the 3D growth on the wider terraces of the SD surface. The growth processes for both surfaces can be described as Volmer–Weber type, but larger islands grow on the SD surface, covering less of the free Si surface, while smaller islands grow on the MD surface, covering more of the free Si surface.

The E_2 bulk critical point for the SD surface is more pronounced than for the MD surface at the same coverage since the Pd growth on the MD surface is more 2D-like than in the SD case. Correspondingly, a larger fraction of the surface is covered by Pd, which reduces the interface signal effectively in particular for high photon energies where the light penetration depth is small.

Structures at 3.55 and 3.6 eV appear for Pd coverages greater than 1 ML, which is close to the E_1 gap of Si and most likely may be related to an interface effect, coming from the reflection at the Pd_2Si/Si interface. Since the total reflection as well as the optical anisotropy of the reflection depends on the contrast in the optical functions of the two media, the growth of Pd_2Si on Si will change the line shape of the optical spectra since the Si/vacuum interface is replaced by a complex Si/Pd_2Si interface.

RAS of the annealed MD surface shows that the peak at 3.65 eV broadens and shifts to 3.75 eV. RAS of the annealed SD surface shows that the amplitude increases towards higher energies with a broad negative anisotropy at energies below 3.5 eV. This is related to the optical anisotropy of crystalline Pd_2Si islands superimposed by light scattering from the rough surface morphology.[32] In summary, RAS spectra and transients clearly demonstrate distinct Volmer–Weber-type growth modes for the MD and SD samples.

Figure 2c shows LEED micrographs of the SD sample. The clean Si(001) surface shows spot splitting indicating long-range order from the double atomic height steps. LEED of the surface with 4 ML Pd is monitored before and after annealing at 600 °C. Split spots that originate from the double height steps are still visible at 4 ML Pd (yellow circle), though the background

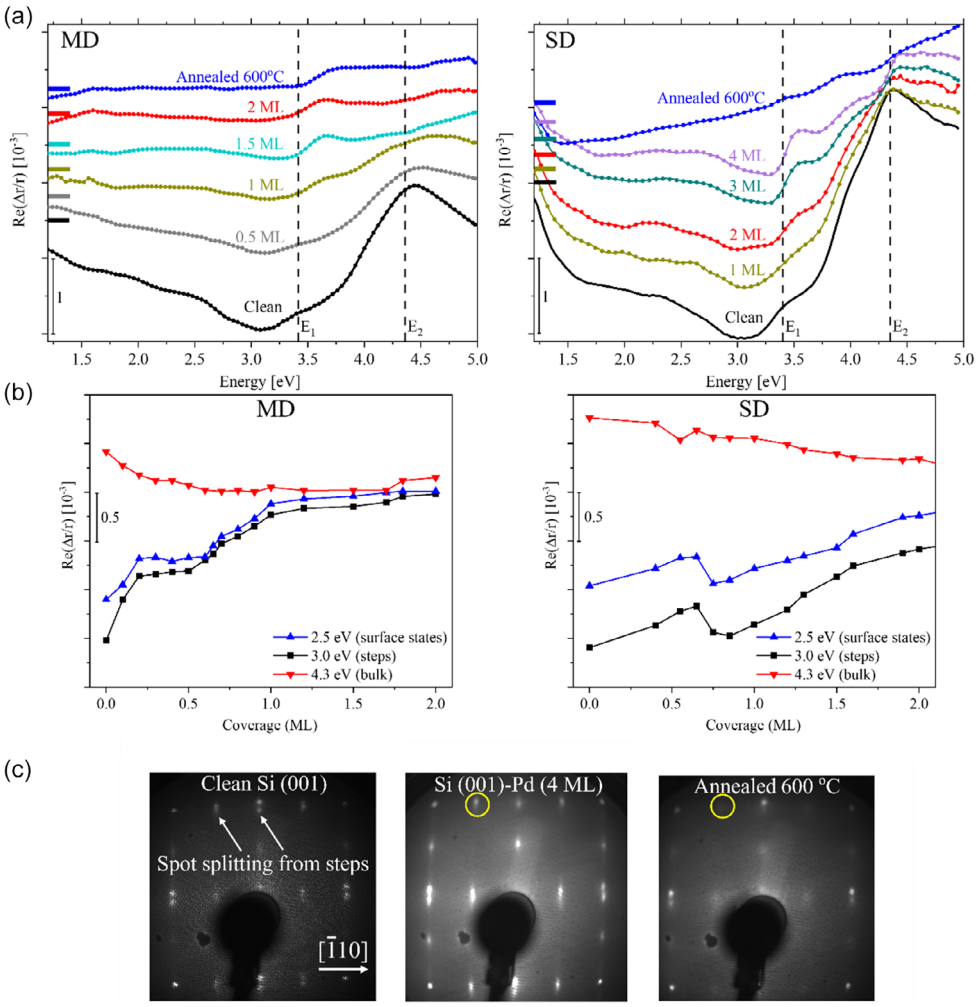

Figure 2. a) RAS of MD and SD Si(001) surfaces at different Pd coverages. The spectra are offset for clarity. Colored bars at the ordinate show zero lines for each coverage. b) RAS transients at different energies representing surface states, steps, and bulk-related transitions versus Pd coverage. c) LEED of the SD clean Si(001) surface, with 4 ML Pd, before and after annealing ($E_{kin} = 54$ eV). Yellow circles indicate the position of a split spot which disappears after annealing.

intensity is higher, indicating increasing disorder. After annealing, some diffuse spots are still present with a reduced number of split spots. LEED of the SD surface supports the RAS data showing that some spot splitting is still observed at higher coverages, indicating the partial presence of the step structure.

RAS of the MD and SD samples are quite different to RAS observed on other silicide structures such as rare earth atoms on vicinal Si(001). There, the metal atoms on the Si surface react strongly by passivating dangling bonds and breaking Si dimers after submonolayer deposition, thus quenching the optical anisotropy.[33] In the case of Pd adsorption, depending on the substrate structure, it seems that it is energetically favorable to initially form islands due to a weaker interaction of Pd with Si.

3.2. Raman Spectroscopy

After each consecutive Pd deposition and RAS measurement, the structural interactions at the interface of Pd and Si were probed with Raman spectroscopy. **Figure 3** shows Raman measurements of the MD and SD samples at RT (unannealed) as well as the difference between the unannealed (I.u) and annealed (I.a) Raman spectra. The spectra at RT are shown in black. Pd itself has no first-order Raman signal. After deposition of Pd, a small peak appears at 116 cm^{-1} for the MD surface. This correlates well with RAS of the same surface which showed a strong reduction in anisotropy. The overall line shape before annealing is mainly related to the density of phonon states of bulk Si. A detailed analysis of the phonon background in this spectral region has been published in our previous work on surface phonons of Si.[19,34]

Several new peaks appear after annealing to 600 °C for 2 min. The Raman spectra were obtained at two different positions, A (light blue) and B (red) on the MD surface, as modes were observed only at specific areas, which indicate inhomogeneous growth. There is a difference in relative peak intensities for the modes seen at 108 cm^{-1} and 116 cm^{-1} at position A and position B. For the SD sample, annealing at 500 °C (dark blue) shows

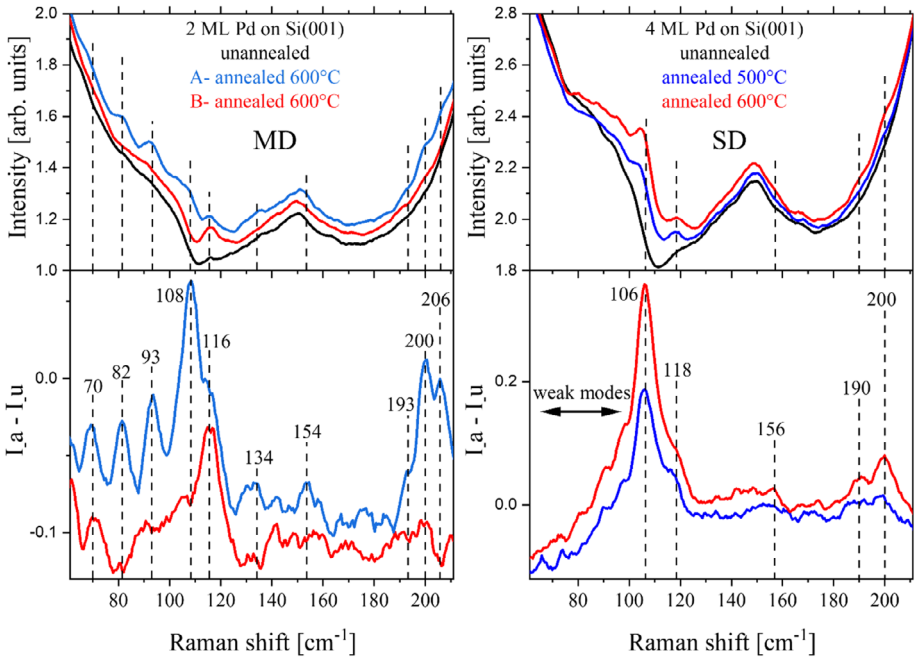

Figure 3. Raman spectroscopy of the MD sample (2 ML Pd) at two positions, A and B—left, and SD sample (4 ML Pd)—right, before annealing (black) and after annealing up to 600 °C. Difference spectra are obtained for the spectra before (I_u) and after (I_a) annealing.

structures appearing at 106 cm^{-1} and at 118 cm^{-1}. The peaks sharpen and increase in intensity, after annealing to 600 °C (red) with some additional weak modes. Pd–Si reaction is clearly visible in the phonon spectra by the appearance of the additional peaks. Nemanich et al. measured Raman spectra for 80 nm-thick Pd films on Si(100).[35] After annealing to 300 °C for 15 min, silicide formation was observed, with a composition near Pd_2Si. The presence of a Pd-rich layer at the top surface was also indicated. After further annealing to 700 °C, a compositionally uniform Pd_2Si silicide was found. The Raman spectra showed groups

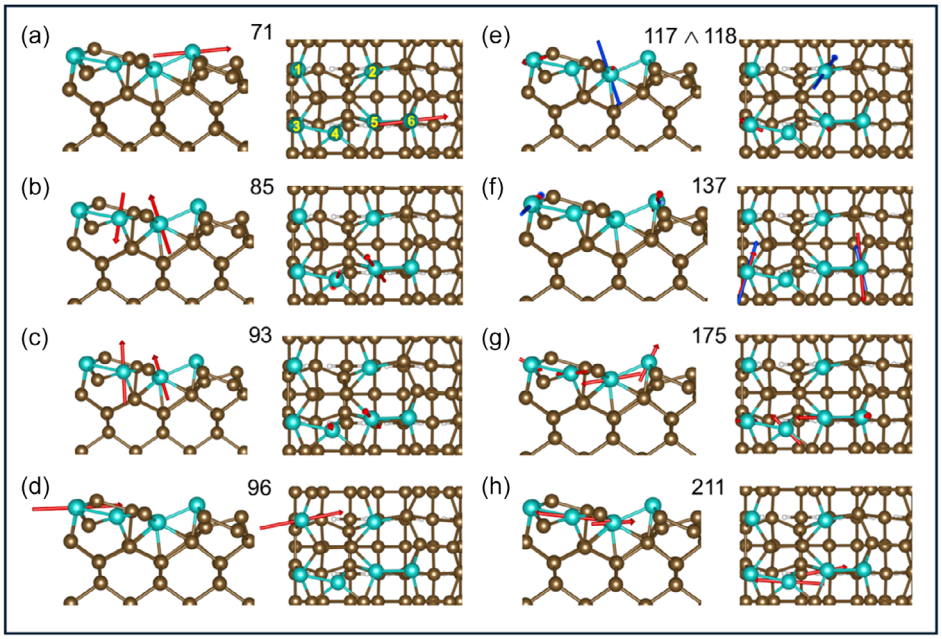

Figure 4. Eigenvectors of the vibrational eigenstates of 6 Pd atoms on a 2 × 1 Si(001) surface, (a–h) that are in good agreement with the phonon modes observed by Raman scattering. For each mode, side and top views are shown. The numbers represent the eigenfrequencies in cm^{-1}. The arrows indicate the direction of the vibrations. For degenerate modes, the second eigenvector is shown by blue arrows.

of lines near those of the initial silicide phase, but at slightly higher frequencies, suggesting the existence of a second phase of Pd_2Si or a similar structure with composition near this. Annealing at 800 °C produced a Raman spectrum of PdSi, which was distinct from that of the two Pd_2Si phases, with the appearance of lines near 150 and 250 cm^{-1}.[35]

Accordingly, the differences in the relative intensities for the 108–116 cm^{-1} peaks may indicate Pd-rich or Pd-poor Pd_2Si phases as suggested by Nemanich.[35] The fact that a small peak is observed at 116 cm^{-1} for the MD sample and a broad shoulder at 118 cm^{-1} for the SD sample before annealing implies some Pd–Si precursor phase for silicide formation, most likely polycrystalline clusters as observed for Pd deposition on Si(111).[12,36] The increased intensity of these structures as well as the appearance of several new peaks between 70 and 200 cm^{-1} after annealing indicates that the chemical interface reaction is promoted upon annealing.

In order to understand the Raman signatures in more detail, ab initio DFT calculations of Pd on Si(001) and respective phonon modes were performed.

Table 1. Calculated and experimentally observed, ν_{exp}, vibrational frequencies of the Pd ad-atoms on a Si(001)-(2 × 1) surface. The calculated frequencies, ν_{theory}, were obtained from force constant calculations employing a harmonic approximation. The measured frequencies, ν_{exp}, were obtained from the in situ Raman scattering experiments shown in Figure 3.

ν_{theory} [cm]$^{-1}$	Remark	ν_{exp}[cm]$^{-1}$
211	In plane stretching of Pd #4 Λ #5 (see Figure 4)	190, 193, 200, 206
175	Stretching of Pd chain #3, #4, #5 Λ #6	–
152	Degenerate out of plane stretching of Pd #1 Λ #2	154, 156
147	Degenerate symmetric and asymmetric out of plane stretching of Pd #3 Λ #6	–
143	–	–
137	Degenerate symmetric and asymmetric in plane wagging of Pd #3 Λ #6	134
128	–	–
117, 118	Degenerate vibration of Pd #2 Λ #3, #5 (see Figure 4)	116, 118
113	–	–
96	In plane wagging of Pd #1 (see Figure 4)	106, 108
93	Symmetric out of plane Pd #4 Λ #5	93
85	Asymmetric out of plane Pd #4 Λ #5	82
71	In plane stretching of Pd #6	70

3.3. DFT Calculations

To address the interface structure and the vibrational modes, DFT calculations were performed for the Si(001)-(2 × 1) surface with a Pd coverage of 75% (**Figure 4**). The Pd ad-atoms destroy the (2 × 1) surface reconstruction and form multiple bonds to silicon atoms of the first two layers. This corresponds well with RAS spectra of the MD sample at 0.5 and 1 ML Pd coverage (Figure 2), where a structure at 3.65 eV, possibly from an intermixed Pd–Si phase, appears. For each Pd atom, the vibrational eigenmodes were calculated. The frequencies are summarized in **Table 1** together with a short description of the observed displacement of the Pd atoms. A number of vibrational modes were observed by Raman spectroscopy that appear to be characteristic for Pd incorporated into a Si(001) surface. Pd atoms incorporate into some lattice sites between the first and second layer, as shown in the calculated minimum energy structure. The experimentally observed modes are in very good agreement with the local vibrational modes obtained from calculations. A comparison to the calculated vibrational modes shows agreement with the eigenmodes between 71 and 211 cm^{-1} (see Table 1). The corresponding modes are depicted in Figure 4, and the direction of the vibrations is indicated by red and blue vectors. These weak features, associated with the reacted Pd–Si-phases at the

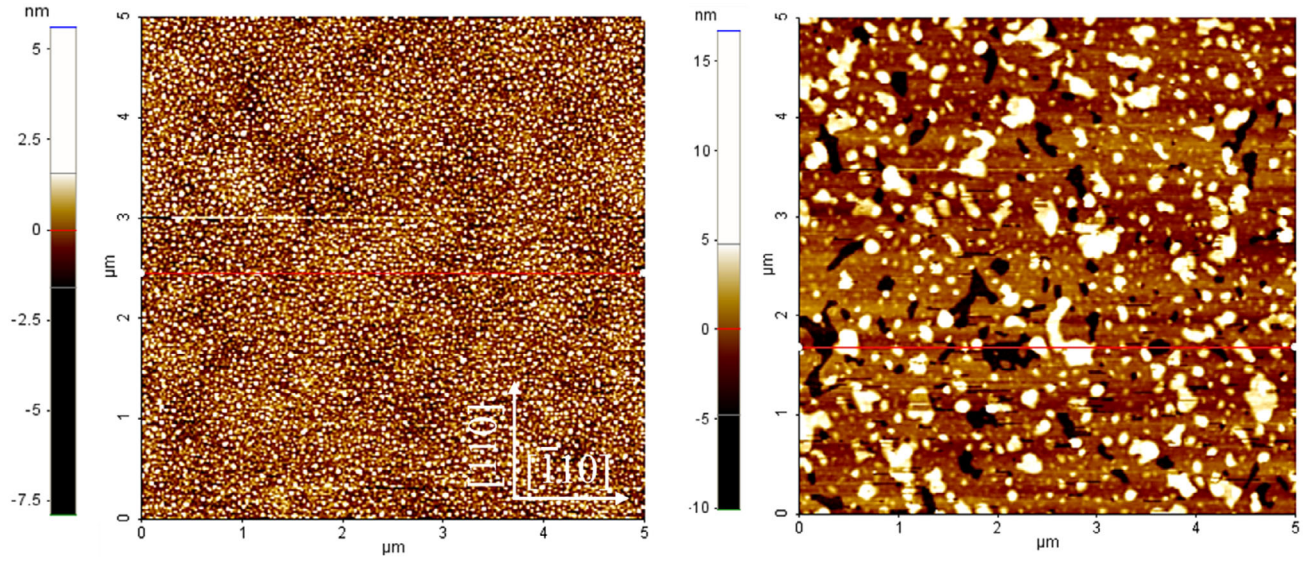

Figure 5. AFM of the MD sample (2 ML Pd and annealing at 600 °C) at two different positions after removal from UHV. The red lines in the AFM images indicate where line profiles were taken but are not included in the figures.

interface, are clearly visible in the experimental Raman spectra, superimposed on the phonon background of the Si substrate; see Figure 3. Thus the comparison of experimental and calculated Raman lines gives clear evidence for the incorporation of Pd atoms into the first Si layer.

4. Ex Situ Measurements (RAS, Raman, and Atomic Force Microscopy (AFM))

As the RAS and Raman results indicated structural differences between the MD and SD sample, the surface morphologies were investigated with AFM in air after removal from UHV. Two types of morphologies are seen for the MD sample (**Figure 5**) at different positions. This agrees well with the Raman measurements performed at different parts of the sample that revealed slightly different vibrational modes in the upper and lower parts of the sample. The high inhomogeneity of the MD sample is probably due to a large temperature gradient during flashing. Exposure to air can induce modification of the structures by producing a complex surface layer which is microscopically inhomogeneous.[37]

A scan size of 5 × 5 μm in one position shows irregular shaped particles roughly 100 nm wide. The average height of the particles is 2 nm. The root mean square roughness is 0.8 nm. In a different position, island formation is seen with much larger sizes of several hundred nm, showing heights of up to 16 nm. The root mean square roughness is 3.8 nm.

AFM images of the SD sample (**Figure 6**a,b,c) are dramatically different. The average heights of the structures range from 4 to 16 nm. Ring-like structures are seen spreading laterally across the surface (Figure 6c), revealing complex textures. The root mean square roughness is ≈2 nm. A close look at Figure 6a shows several small, rod-like structures oriented along the <110> direction which could indicate the formation of Pd–Si islands. Concentric ring formations can be seen in Figure 6c.

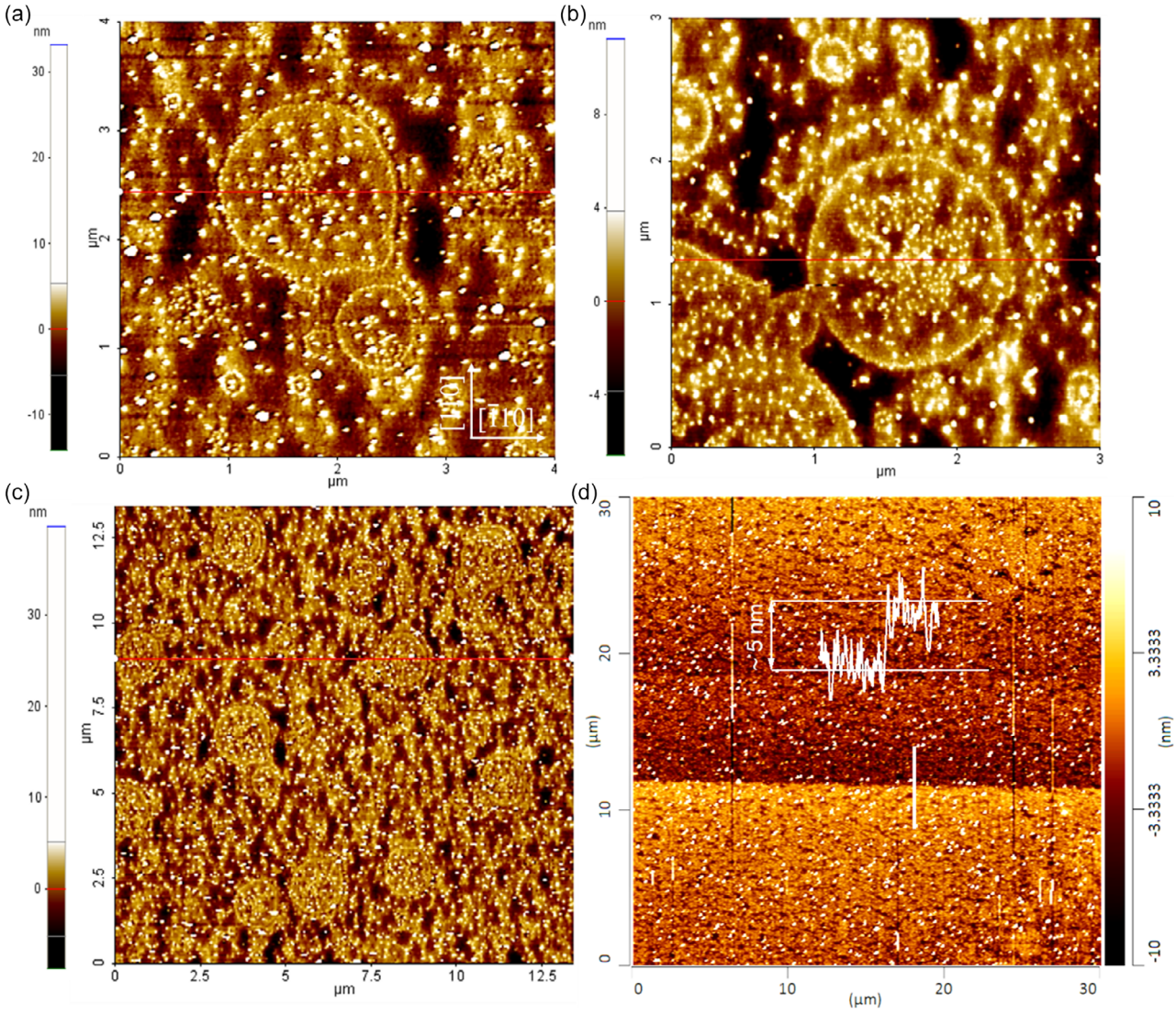

Figure 6. a,b,c) AFM of the SD sample (4 ML Pd and annealing at 600 °C) after removal from UHV. d) AFM micrograph showing long straight steps due to faceting, with a line scan (white line) across the steps (inset) showing height profile of 5 nm.

Studies on the kinetics and morphology of phase transformations in Pd silicides have observed that some silicides are formed by nucleation at defects or impurities, followed by lateral growth away from these nucleation centers.[38] Nucleation-controlled kinetics are observed in many metal-silicon complexes.[39–41] It typically takes place when one silicide phase (previously formed at lower temperatures in the thermal annealing) reacts with the silicon substrate to form another silicide phase. Silicides formed by this process often exhibit wavy surface morphologies.[39] Upon further heating, nucleation centers appear all over the surface and grow until they coalesce into colonies.[38]

An AFM micrograph of a larger scan area is shown in Figure 6d where extremely long steps are seen with a height of 5 nm. Step bunching of very regular, straight double steps with a height of 0.27 nm can lead to faceting after metal deposition (multiples of this height would result in steps of ≈5 nm).

Figure 7 shows ex situ RAS measurements on the MD and SD samples. RAS of the MD sample shows that some broad features close to the E_1 and E_2 critical points are still visible. RAS of the SD sample shows some small features near E_1 and E_2, but the spectrum is mostly isotropic. Since the MD sample has a smaller coverage of Pd compared to the SD sample, the Si interface signal is still visible compared to the SD sample. Ex situ AFM of the SD sample showed mostly circular structures which could explain the isotropic nature of the RAS signal. We would like to note that the E_1 and E_2 structures must originate from the Pd_2Si/Si interface since the free Si surface areas are oxidized and show a flat RAS spectrum.

Figure 8 shows ex situ Raman spectra of the MD and SD samples, measured at an excitation wavelength of 457 nm. A small feature near 256 cm^{-1} is seen for both samples. Nemanich et al. had shown that a PdSi phase can be produced by annealing a Pd_2Si sample at 800 °C with the appearance of lines near 250 cm^{-1}.[35] The small feature at 256 cm^{-1} for the ex situ Raman spectra could indicate the appearance of this PdSi phase. The SD sample shows a sharper and larger amplitude at 256 cm^{-1} compared to the MD sample. This could be due to the thicker layer of Pd in the SD sample. The corresponding 2TA mode for Si at 300 cm^{-1} is also reduced for the SD sample. The appearance of the features near 256 cm^{-1} for the ex situ Raman spectra indicates that a PdSi related phase is still present after several months in atmosphere.

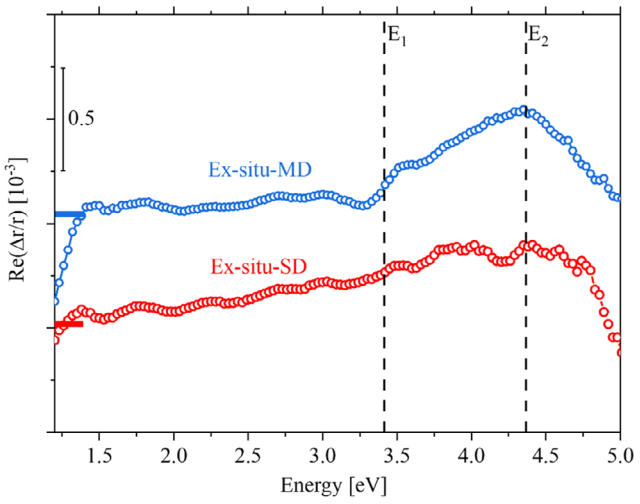

Figure 7. Ex situ RAS of the MD (2 ML Pd, annealed at 600 °C) and SD (4 ML, annealed at 600 °C) samples after removal from UHV and storage in air for 90 days.

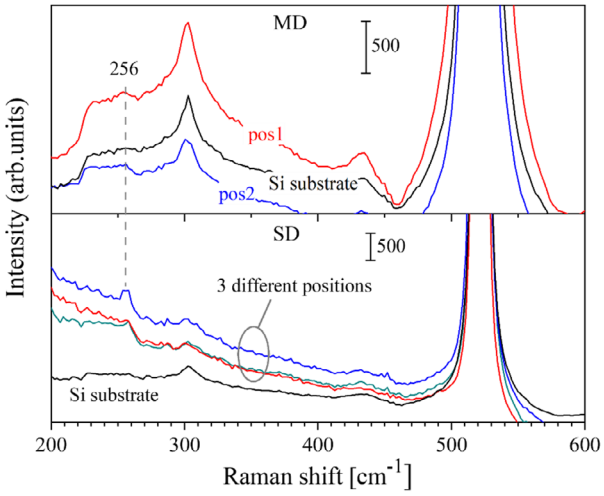

Figure 8. Ex situ Raman of the MD (2 ML Pd, annealed at 600 °C) and SD (4 ML, annealed at 600 °C) samples after removal from UHV and storage in air for 90 days.

5. Summary

The early stage reactions of Pd atoms on the Si(001) surface were investigated using RAS and Raman scattering. The silicidation process has been shown to be influenced by the initial interactions between palladium and silicon. RAS monitored the precursor state of Pd silicidation and showed that, depending on the Si surface structure, Pd does not initially passivate the majority of the dangling bonds on the Si dimers or steps as seen for rare earth atoms but prefers to diffuse into the Si surface. The formation of small amounts of Pd on vicinal Si(001) can thus be investigated with RAS, by monitoring the initial stages of island growth which form a Pd–Si precursor state.

Raman spectroscopy and DFT calculations provide clear evidence of the formation of a surface alloy during the deposition process, where Pd adsorbs and inserts into the clean Si(100) subsurface with the calculated modes agreeing well with the experimentally observed vibrational modes.

Raman spectra show initial reacted phases of Pd–Si which are in good agreement with a complex structure caused by incorporation of Pd in the upper two Si layers. The initial adsorption of Pd on the silicon substrate and the formation of the interface mixed layer are shown to be strongly influenced by the surface step structure.

Depending on the surface structure, AFM measurements showed either nonuniform films with islands or circular wave-like features due to nucleation-controlled reactions. Ex situ Raman measurements showed some weak, broad features which could be related to the appearance of a PdSi phase after removal from UHV.

The extremely dilute amounts of Pd on the Si(001) surface in this work could be tested in future studies for catalytic activity since Si-modified Pd catalysts have shown improved performance due to the geometric modification of the Pd surface by Si.[42]

Acknowledgements

S.C. acknowledges support from the Federal Ministry of Education and Research in the framework of the project CatLab (03EW0015A/B). K.H. acknowledges support from the EFRE project 1.8/13. N.E. acknowledges support from the EFRE project 1.8/07. The authors thank Özgür Savaş at HZB for the AFM measurements.

Open Access funding enabled and organized by Projekt DEAL.

Conflict of Interest

The authors declare no conflict of interest.

Data Availability Statement

The data that support the findings of this study are available from the corresponding author upon reasonable request.

Keywords

density functional theory, morphologies, optical, palladium, silicon, silicide, vibrational

Received: December 12, 2024
Revised: February 17, 2025
Published online: March 31, 2025

[1] L. J. Chen, *JOM* **2005**, *57*, 24.
[2] K. N. Tu, J. W. Mayer, *Thin Films-Interdiffusion And Reactions*, Wiley, New York **1978**, p. 359.
[3] M. A. Nicolet, S. S. Lau, *Materials Process and Characterization*, Academic, New York **1983**, p. 329.
[4] A. Borodziński, G. C. Bond, *Catalysis Rev.* **2006**, *48*, 91.
[5] M. Chen, D. Kumar, C.-W. Yi, D. W. Goodman, *Science* **2005**, *310*, 291.
[6] Z. Li, E. Öztuna, K. Skorupska, O. V. Vinogradova, A. Jamshaid, A. Steigert, C. Rohner, M. Dimitrakopoulou, M. J. Prieto, C. Kunkel, M. Stredansky, *Nat. Commun.* **2024**, *15*, 10660.
[7] C. Calandra, O. Bisi, G. Ottaviani, *Surf. Sci. Rep.* **1985**, *4*, 271.
[8] G.A. Hutchins, A. Shepela, *Thin Solid Films* **1973**, *18*, 343.
[9] R. M. Tromp, E. J. van Loenen, M. Iwami, R. G. Smeenk, F. W. Saris, F. Nava, G. Ottaviani, *Surf. Sci.* **1983**, *124*, 1.
[10] H. Itoh, S. Narui, H. Tanabe, T. Ichinokawa, *Surf. Sci.* **1993**, *284*, 236.
[11] K. N. Tu, *J. Appl. Phys.* **1982**, *53*, 428.
[12] L. Casalis, C. Casati, R. Rosei, M. Kiskinova, *Surf. Sci.* **1995**, *331–333*, 381.
[13] B. Y. Tsaur, M-A. Nicolet, *Appl. Phys. Lett.* **1980**, *37*, 708.
[14] O. Bisi, K. N. Tu, *Phys. Rev. Lett.* **1984**, *52*, 1633.
[15] T. Zambelli, J. Wintterlin, J. Trost, G. Ertl, *Science* **1996**, *273*, 1688.
[16] B. Hammer, O. H. Nielsen, J. K. Nrskov, *Catal. Lett.* **1997**, *46*, 31.
[17] L.Q. Lee, P.L. Cao, *J. Phys. Condens. Matter* **1996**, *8*, 3313.
[18] C. Hogan, E. Speiser, S. Chandola, S. Suchkova, J. Aulbach, J. Schäfer, S. Meyer, R. Claessen, N. Esser, *Phys. Rev. Lett.* **2018**, *120*, 166801.
[19] S. Sanna, J. Plaickner, K. Holtgrewe, V. M. Wettig, E. Speiser, S. Chandola, N. Esser, *Materials* **2021**, *14*, 4104.
[20] E. Speiser, N. Esser, B. Halbig, J. Geurts, W. G. Schmidt, S. Sanna, *Surf. Sci. Rep.* **2020**, *75*, 100480.
[21] D. E. Aspnes, A. A. Studna, *Phys. Rev. Lett.* **1985**, *54*, 1956.
[22] K. Fleischer, S. Chandola, Th Herrmann, N. Esser, W. Richter, J. F. McGilp, *Phys. Rev. B* **2006**, *74*, 195432.
[23] G. Kresse, J. Furthmüller, *Phys. Rev. B* **1996**, *54*, 11169.
[24] G. Kresse, J. Joubert, *Phys. Rev. B* **1999**, *59*, 1758.
[25] J. Perdew, K. Burke, M. Ernzerhof, *Phys. Rev. Lett.* **1996**, *77*, 3865.
[26] Y. Borensztein, N. Witkowski, S. Royer, *Phys. Status Solidi C* **2003**, *0*, 2966.
[27] N. Witkowski, R. Coustel, O. Pluchery, Y. Borensztein, *Surf. Sci.* **2006**, *600*, 5142.
[28] W. G. Schmidt, F. Bechstedt, J. Bernholc, *Phys. Rev. B* **2001**, *63*, 045322.
[29] S. G. Jaloviar, J.-L. Lin, F. Liu, V. Zielasek, L. McCaughan, M. G. Lagally, *Phys. Rev. Lett.* **1999**, *82*, 791.
[30] D. Papadimitriou, W. Richter, *Phys. Rev. B* **2005**, *72*, 075212.
[31] K. Hingerl, R.E. Balderas-Navarro, A. Bonanni, P. Tichopadek, W.G. Schmidt, *Appl. Surf. Sci* **2001**, *175–176*, 769.
[32] M. Amiotti, G. Guizzetti, F. Marabelli, A. Piaggi, V. N. Antonov, Vl. N. Antonov, O. Jepsen, O. K. Andersen, A. Borghesi, F. Nava, V. V. Nemoshkalenko, R. Madar, A. Rouault, *Phys. Rev. B* **1992**, *45*, 13285.
[33] S. Chandola, E. Speiser, N. Esser, S. Appelfeller, M. Franz, M. Dähne, *Appl. Surf. Sci.* **2017**, *399*, 648.
[34] E. Speiser, J. Plaickner, S. Chandola, N. Esser, B. Halbig, J. Geurts, *Phys. Status Solidi B* **2019**, *256*, 1800341.
[35] R. J. Nemanich, C. C. Tsai, T. W. Sigmon, *Phys. Rev. B* **1981**, *23*, 6828.
[36] U. K. Köhler, J. E. Demuth, R. J. Hamers, *Phys. Rev. Lett.* **1988**, *60*, 2499.
[37] A.J. Brunner, A. Stemmer, L. Rosenthaler, R. Wiesendanger, M. Ringger, P. Oelhafen, H. Rudin, H.-J. Güntherodt, *Surf. Sci.* **1987**, *181*, 313.
[38] C. S. Wei, J. Van der Spiegel, J. Santiago, *J. Appl. Phys.* **1985**, *58*, 4200.
[39] P. Gas, F. M. d'Heurle, F. K. LeGoues, S. J. La Placa, *J. Appl. Phys.* **1986**, *59*, 3458.
[40] R. Anderson, J. Baglin, J. Dempsey, W. Hammer, F. d'Heurle, S. Petersson, *Appl. Phys. Lett.* **1979**, *35*, 285.
[41] C. A. Dimitriadis, J. H. Werner, *J. Appl. Phys.* **1990**, *68*, 93.
[42] E. W. Shin, C. H. Choi, K. S. Chang, Y. H. Na, S. H. Moon, *Catal. Today* **1998**, *44*, 137.